Supporting Information: Reaction Mechanism for Methane-to-Methanol in Cu-SSZ-13: First-Principles Study of the $Z_2[Cu_2O]$ and $Z_2[Cu_2OH]$ Motifs

Unni Engedahl,* Adam A. Arvidsson, Henrik Grönbeck, and Anders Hellman*

Department of Physics and Competence Centre for Catalysis, Chalmers University of Technology, Gothenburg

E-mail: unni@chalmers.se; anders.hellman@chalmers.se

Molecular vibrations

The structural properties of gas-phase H_2O, CH_4, and CH_3OH are in good agreement with experimental values, as seen in table S1.

Table S1: Vibrational frequencies for H_2O, CH_4, and CH_3OH. Comparison between calculated and experimental values, all in cm^{-1}.

H_2O		CH_4		CH_3OH	
Calc.	Exp.	Calc.	Exp.	Calc.	Exp.
1582	1595	1271	1306	289	200
3697	3657	1275	1306	1005	1033
3806	3756	1279	1306	1033	1060
		1502	1534	1095	1165
		1503	1534	1325	1345
		2942	2917	1385	1455
		3055	3019	1432	1477
		3057	3019	1447	1477
		3058	3019	2839	2844
				2923	2960
				3011	3000
				3719	3681

Vibrational frequencies of reaction intermediates

The vibrational frequencies of the reaction intermediates in the zeolites Z[Cu_2O] and Z[Cu_2OH] are found in table S2.

Table S2: Vibrational frequencies for reaction intermediates in Z[Cu_2O], all in cm^{-1}. For each intermediate, the copper atoms of the active site are included in the vibrational analysis.

*O	*O,CH_4	TS1	*OH,CH_3	TS2	*CH_3OH	CH_3OH,H_2O	*	*H_2O	*H_2O,H_2O
10.0	10.0	10.0	46.8	10.0	10.0	10.0	54.0	72.5	10.0
10.0	10.0	10.0	59.7	10.0	10.0	10.0	60.0	86.5	37.4
10.0	10.0	10.0	67.1	34.0	10.0	37.0	138.4	100.6	66.1
62.5	10.0	10.0	109.9	62.0	82.8	65.0	158.9	135.9	71.2
93.8	10.0	93.8	120.7	103.9	108.5	81.7	188.1	177.1	84.8
122.3	62.6	98.1	146.3	125.3	113.6	94.5	235.1	221.1	119.4
142.8	117.9	107.7	169.1	130.1	132.3	113.6		251.7	150.5
206.8	138.7	131.4	209.0	199.8	161.9	125.3		326.7	174.3
243.8	186.3	163.8	233.4	230.3	208.5	156.7		491.5	179.9
	197.6	174.1	279.7	339.1	244.9	166.9		541.8	220.9
	208.4	209.5	410.0	489.1	247.3	186.0		743.7	256.9
	212.5	259.8	424.4	612.3	392.9	202.2		1172.0	277.0
	312.8	528.4	560.4	741.0	1043.2	224.4		1556.6	310.0
	603.0	571.7	698.1	795.6	1158.0	265.4		2051.3	314.3
	708.0	722.7	730.9	868.9	1190.5	447.2		3637.6	466.2
	1264.6	826.1	1077.4	1056.7	1227.1	473.8			525.4
	1270.6	1073.9	1097.7	1158.8	1428.8	545.8			711.0
	1279.7	1163.1	1149.2	1341.3	1435.0	723.1			1100.2
	1494.6	1393.4	1350.7	1392.4	1445.2	966.5			1553.6
	1497.2	1656.0	1367.4	2919.4	1476.0	1172.4			1570.2
	2932.5	2885.5	2775.8	2977.2	2501.4	1188.7			2394.1
	3023.8	3793.6	2872.8	3077.4	2944.8	1252.8			3622.8
	3057.1	4607.7	2974.3	3140.7	3030.4	1412.3			3673.5
	3100.3		3070.7		3078.5	1438.9			3737.4
						1453.7			
						1456.7			
						1557.9			
						2602.2			
						2894.3			
						2968.4			
						3069.9			
						3458.6			
						3648.1			

Table S3: Vibrational frequencies for reaction intermediates in Z[Cu_2OH], all in cm^{-1}. For each intermediate, the copper atoms of the active site arer included in the vibrational analysis.

*OH	*OH,CH_4	TS1	*CH_3OH,H	*CH_3,H_2O	CH_3OH,H,H_2O	*H	*H,H_2O	*H,2(H_2O)
123.0	100.0	100.0	100.0	100.0	100.0	100.0	100.0	100.0
140.1	100.0	100.0	100.0	100.0	100.0	125.3	100.0	100.0
167.3	100.0	100.0	116.4	100.0	100.0	153.1	122.3	100.0
195.8	100.0	100.0	125.2	100.0	100.0	155.7	129.8	100.0
216.4	100.0	124.5	138.4	110.1	100.0	212.1	156.1	100.0
249.2	100.0	127.2	162.2	130.6	100.0	285.8	186.8	103.2
465.9	117.5	177.1	176.8	162.9	101.3	316.4	204.8	117.9
541.3	147.3	180.6	184.4	167.4	119.8	1292.0	250.6	119.8
1063.0	159.9	198.3	191.4	169.5	136.1	1502.8	350.6	161.9
1513.2	162.0	200.6	218.8	250.8	155.5		370.9	178.7
1649.6	197.1	214.5	247.1	314.8	167.3		494.3	200.2
3280.1	203.8	233.1	325.8	357.6	181.0		621.2	216.4
	245.1	338.2	450.4	383.6	211.4		987.8	301.9
	543.4	480.6	852.2	521.9	314.8		1387.9	354.1
	612.1	620.0	966.4	616.1	355.8		1529.3	450.3
	798.1	654.8	1105.2	697.7	385.4		1538.9	612.7
	982.9	767.8	1123.2	700.8	422.8		2758.1	653.2
	1271.9	1109.0	1349.6	777.9	537.4		3679.0	662.5
	1274.9	1344.2	1384.9	1224.3	605.7			762.6
	1278.1	1351.0	1413.1	1268.1	778.8			1056.1
	1492.6	1546.1	1429.8	1405.3	956.0			1494.0
	1497.1	2338.4	1441.7	1545.8	1078.6			1541.2
	2925.0	2982.2	1561.5	2586.7	1118.0			1605.9
	3029.2	3156.9	2902.5	2885.3	1262.9			2115.5
	3032.5	3170.6	2989.6	3039.5	1309.6			3465.6
	3067.1	3501.5	3014.5	3251.9	1408.1			3939.4
	3258.7		3048.5	3664.0	1427.1			4008.1
					1439.0			
					1597.5			
					1654.3			
					2930.1			
					3013.6			
					3041.5			
					3334.7			
					3479.1			
					3588.1			

Zeolite framework

The chabazite framework SSZ-13 is a small pore zeolite with 4, 6, and 8 membered rings (MRs). The smallest unit cell consists of 12 T-site, here distributed as 10 SiO_4 and 2 AlO_4 sites, as seen in fig. S1a). On a larger scale, the framework is made up of two different sized cages, shown in fig. S1b).

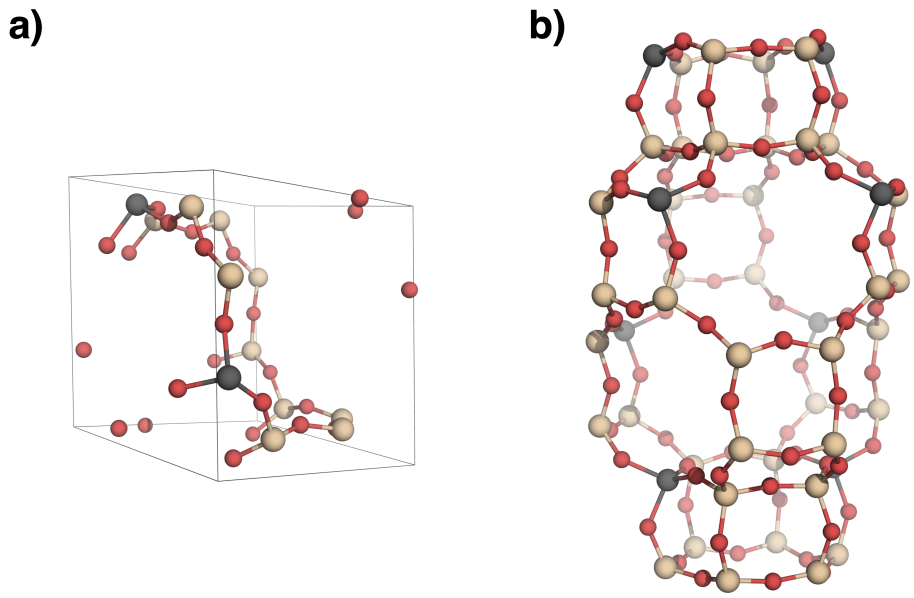

Figure S1: The zeolite system SSZ-13 has 4/6/8 MRs. a) shows the smallest unit cell consisting of 12 T-sites, and b) exhibits one large and two small cages of the SSZ-13 structures.

Reaction mechanism over $Z_2[Cu_2O]$

Energy landscape

The reaction mechanism over $Z_2[Cu_2O]$ in relative energy is found in fig. S2. The dry reaction path, marked by red squares, is endothermic. However, with addition of water to the reaction mechanism, the reaction becomes exothermic (blue crosses in fig. S2).

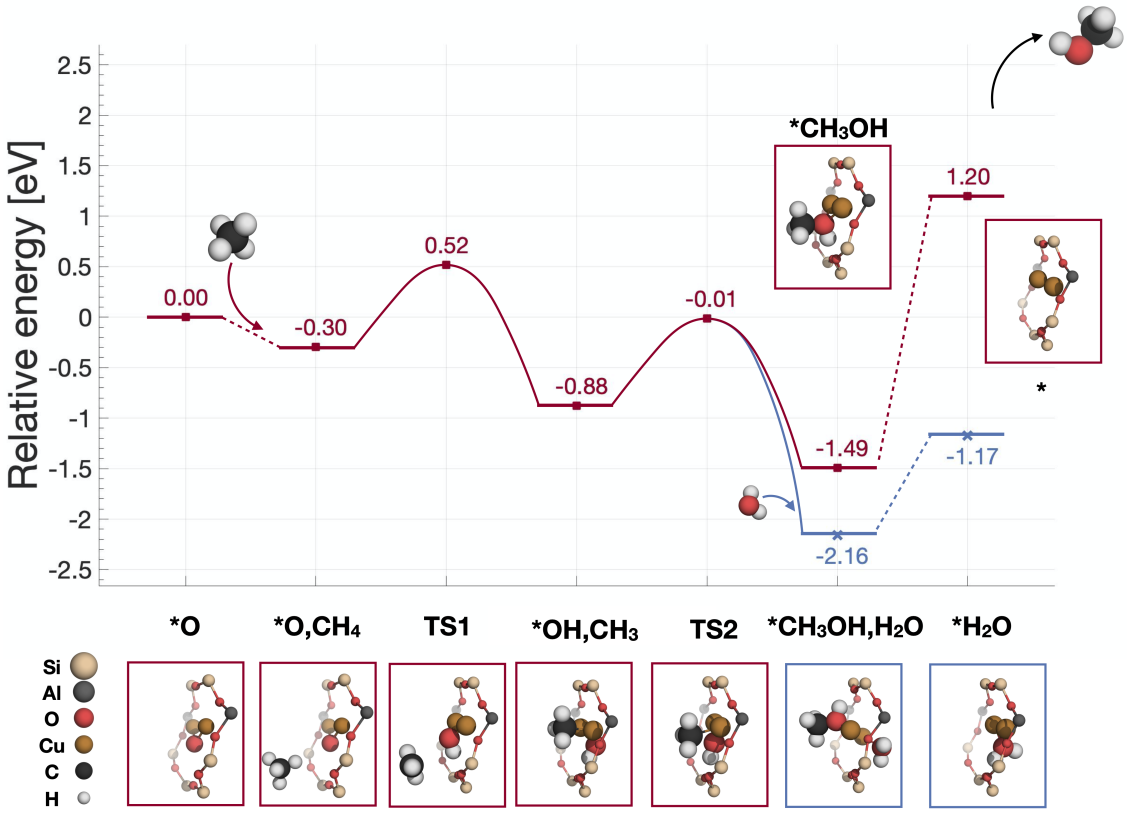

Figure S2: Reaction mechanism in relative energies for $Z_2[Cu_2O]$. The dry reaction mechanism is that with red squares, with one water is blue crosses, and with two water is a black dot. Energies are in eV.

Effect of +U correction

The reaction mechanism over $Z_2[Cu_2O]$ in relative energy is found in fig. S3. The dry reaction paths are marked by squares, and crosses mark when water is added to the mechanism. Over all, the addition of a +U correction of U=6 eV increases the adsorption energy of the reactants and lowers the energy of CH_3OH desorption.

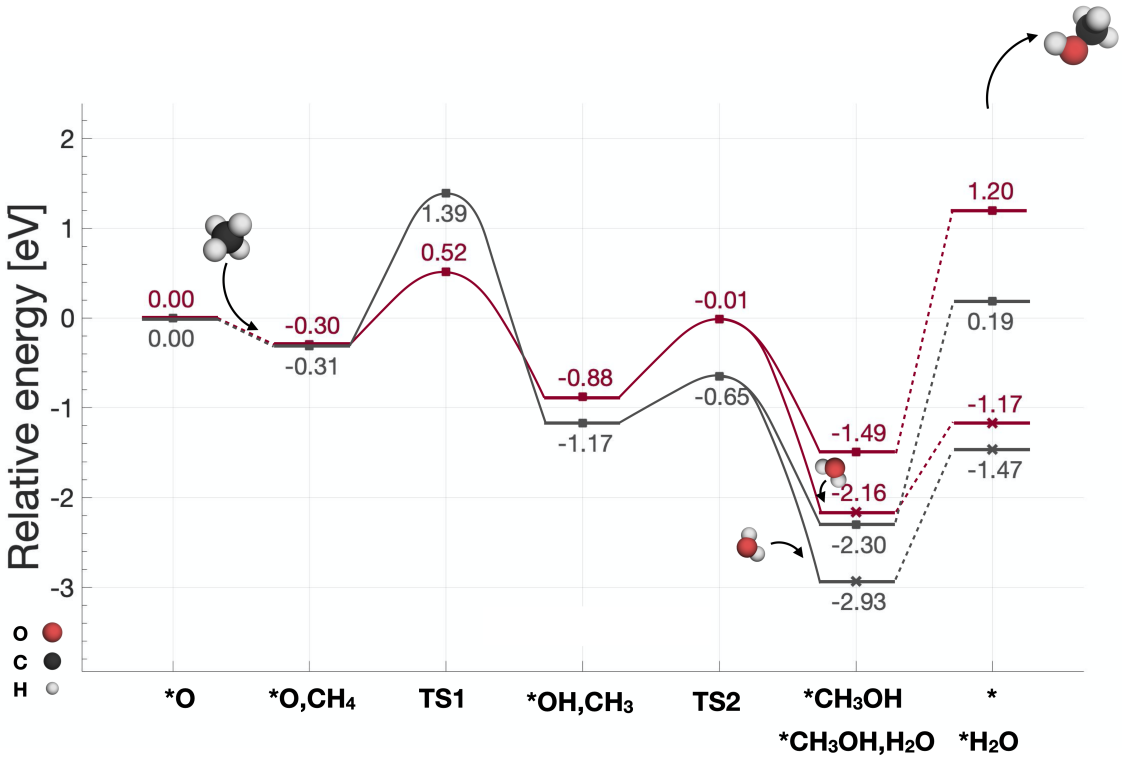

Figure S3: Reaction mechanism in relative energies, with and without a +U correction, for $Z_2[Cu_2O]$. The red path shows the energy without +U correction and the gray shows the energy with the correction. Squares show the paths where no water is present and the crosses include H_2O. Energies are in eV.

Gas-phase molecules inside the zeolite

When gas-phase molecules are present in the zeolite cage, their entropy contribution is affected by the confinement of the zeolite structure according to

$$S^{zeo} = \frac{2}{3}\left(S^{gas}_{trans} + S^{gas}_{rot}\right) + S^{zeo}_{vib}, \tag{1}$$

where S^{gas}_{trans} and S^{gas}_{rot} are entropy contributions from the gas phase translations and rotations of the molecule, and S^{zeo}_{vib} is the entropy contribution from the vibrational modes of the molecule.

Treating CH_4 as a gas-phase species in $Z_2[Cu_2O]$ decreases the Gibbs free energy as seen in fig. S4, where the *O,CH_4 intermediate is calculated either in gas-phase (dashed line with ΔG=0.28 eV)or in the harmonic approximation (dotted line with ΔG 0.45 eV higher in energy). Both treatments result in an endergonic inclusion of CH_4 to the system.

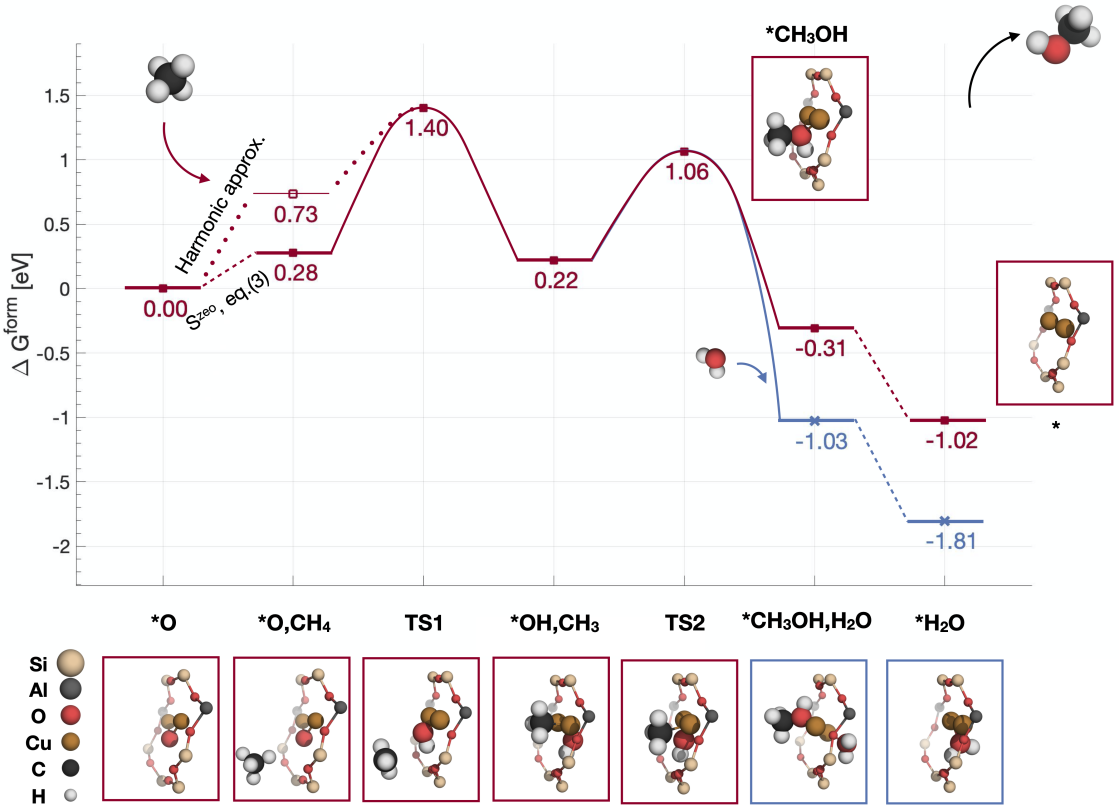

Figure S4: Reaction mechanism over $Z_2[Cu_2O]$. Treated in the harmonic approximation, the change in free energy of the $*O,Ch_4$ intermediate is 0.28 eV, and treated as a gas-phase species in the zeolite according to eq. (1), it is 0,73 eV. Reaction conditions are set to T=448 K, p_{CH_4}=2%, p_{H_2O}=10%, and p_{CH_3OH}=10^{-9}%, with respect to atmospheric pressure. All energies are in eV.

Reaction mechanism over $Z_2[Cu_2OH]$

Energy landscape

The energy landscape of the reaction mechanism over $Z_2[Cu_2OH]$ is found in fig. S5. The dry reaction path marked by purple diamonds, as well as the path including water (blue crosses), is endothermic.

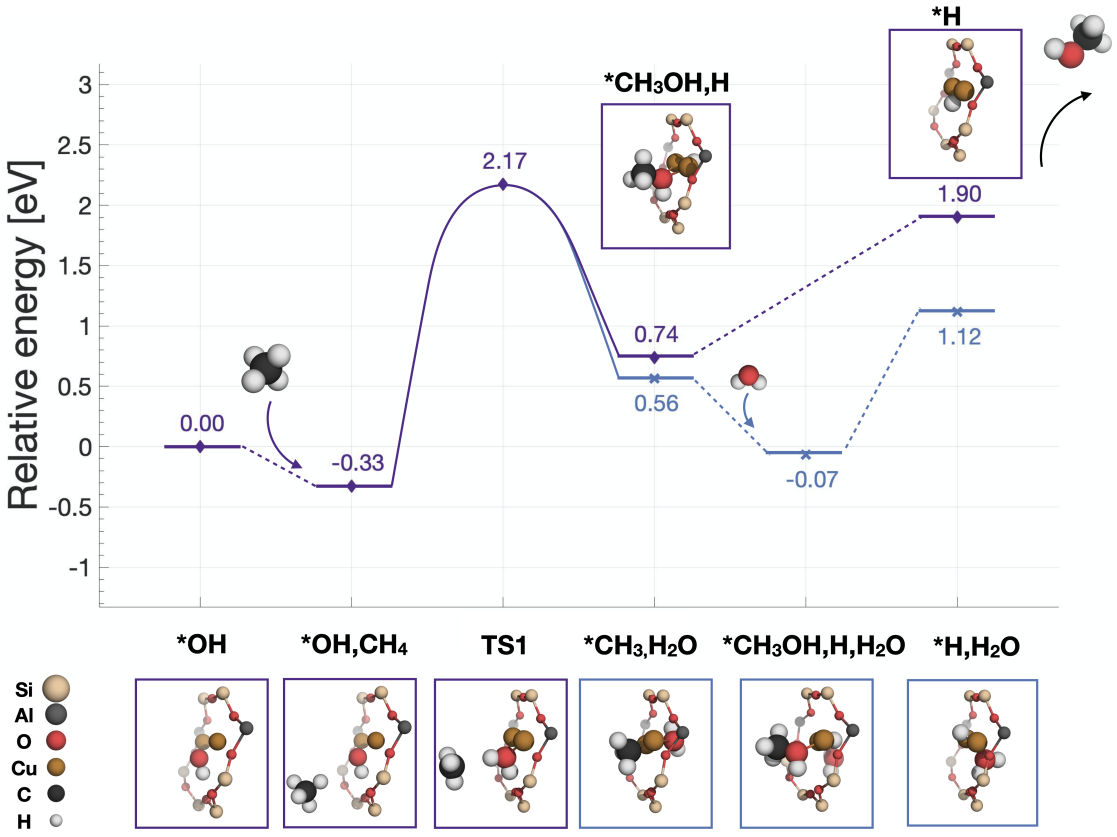

Figure S5: Reaction mechanism in relative energies for $Z_2[Cu_2OH]$. The dry reaction mechanism is that with purple diamonds. The path including water is marked by blue crosses. Energies are in eV.

Effect of +U correction

The energy landscape over $Z_2[Cu_2OH]$ in relative energy, with and without a +U correction of U=6 eV, is found in fig. S6, as purple and gray paths, respectively. The dry reaction paths are marked by squares, and crosses mark when water is added to the mechanism. The +U correction has a smaller effect on the $Z_2[Cu_2OH]$ system than on the $Z_2[Cu_2O]$ structure. Notably, the energy of the CH_3OH desorption in the dry path is increased rather than decreased when adding the correction.

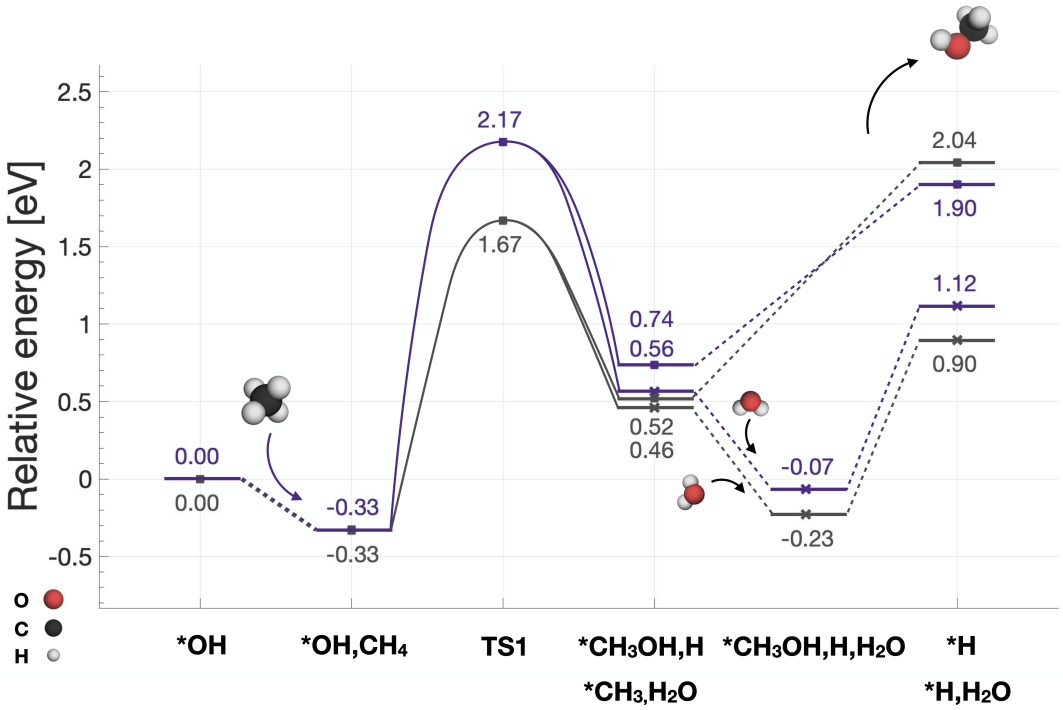

Figure S6: Reaction mechanism in relative energies, with and without a +U correction, for $Z_2[Cu_2OH]$. The purple path shows the energy without the +U correction and the gray shows the energy with the correction. Squares show the paths where no water is present, and the crosses include H_2O. Energies are in eV.

Gas-phase molecules inside the zeolite

As for $Z_2[Cu_2O]$, the *O,CH_4 intermediate in the $Z_2[Cu_2OH]$ system is stabilized when CH_4 is treated as a gas-phase species inside the zeolite. The dashed line in fig. S7 is 0.46 eV lower in energy when compared to the dotted line marking the system treated with the harmonic approximation. Interestingly, in $Z_2[Cu_2OH]$ treatment according to eq. (1) results in a exergonic inclusion of CH_4. This differs from $Z_2[Cu_2O]$, where the addition of CH_4 is stabilized but still endergonic.

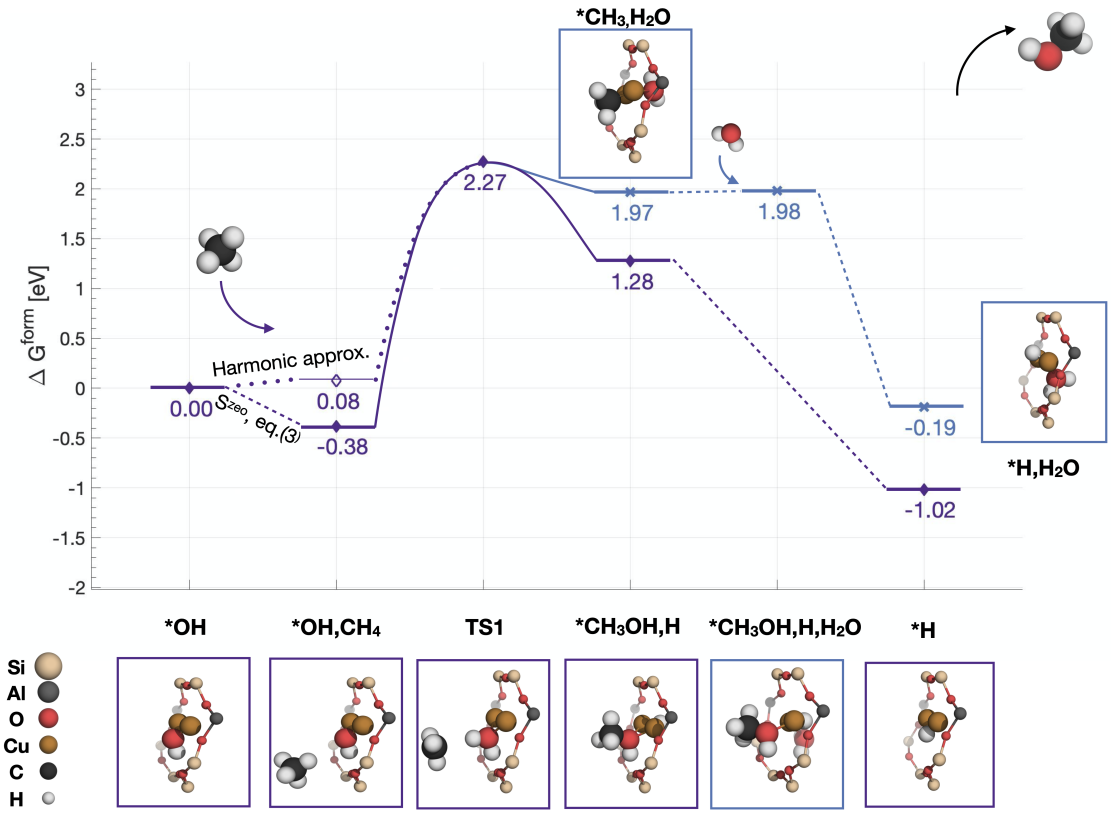

Figure S7: Reaction mechanism over $Z_2[Cu_2OH]$ where gas-phase CH_4 in the zeolite is treated in two different ways. Treated in the harmonic approximation, the change in free energy of the *O,Ch_4 intermediate is 0.08 eV, and treated as a gas-phase species in the zeolite according to eq. (1), $\Delta G = -0.38$ eV. Reaction conditions are set to T=448 K, p_{CH_4}=2%, p_{H_2O}=10%, and p_{CH_3OH}=10^{-9}%, with respect to atmospheric pressure. All energies are in eV.

Micro-kinetic model

In fig. S8 the effect of the two different treatments of reactants (as gas-phase species or as adsorbates in the zeolite) on the transient kinetics of the reaction over the $Z_2[Cu_2O]$ and $Z_2[Cu_2OH]$ sites in SSZ-13, as well as over the $Z_2[Cu_2O]$ site in the large pore zeolite ZSM-5, is shown. The time needed for conversion of the active sites into CH_3OH is shown in fig. S8a), where the only system affected by the change in treatment of the reactants is the Cu_2OH system. However, the dashed line showing the harmonic treatment in fig. S8a) still shows very poor performance. Halftime of the sites as a function of temperature is shown in fig. S8b). The two highest performing systems, $Z_2[Cu_2O]$ZSM-5 and $Z_2[Cu_2O]H_2O$ SSZ-13, show little change with increasing temperature, while the poor performing systems shows a clear increase in activity when the temperature is increased. As for fig. S8a), the increase in activity caused by the harmonic treatment is not significant enough to change the relative order of the sites when it comes to the activity of the systems.

Coverages

In fig. S9, coverages for the two different treatments of the entropy contribution to the free energy are found. Again, the $Z_2[Cu_2OH]$ in SSZ-13 differs the most between the methods. In gas phase, the adsorption of CH_4 becomes exergonic (see fig. S7), causing the *OH,CH_4 site to cover the structure from 10^{-7} s to 10^{15} s. $Z_2[Cu_2O]$ in SSZ-13, on the other hand, does not show the same sensitivity to the choice of method.

Reaction mechanism over Cu-ZSM-5

The energy landscape of the reaction mechanism over $Z_2[Cu_2O]$ in the MFI zeolite ZSM-5 is compared to that of $Z[Cu_2O]$ in SSZ-13 in fig. S10. Dry reaction conditions apply. The mechanism follows the same general pattern in their respective frameworks. MFI (yellow dots in fig. S10) having lower barriers throughout the reaction, most so in the last step of

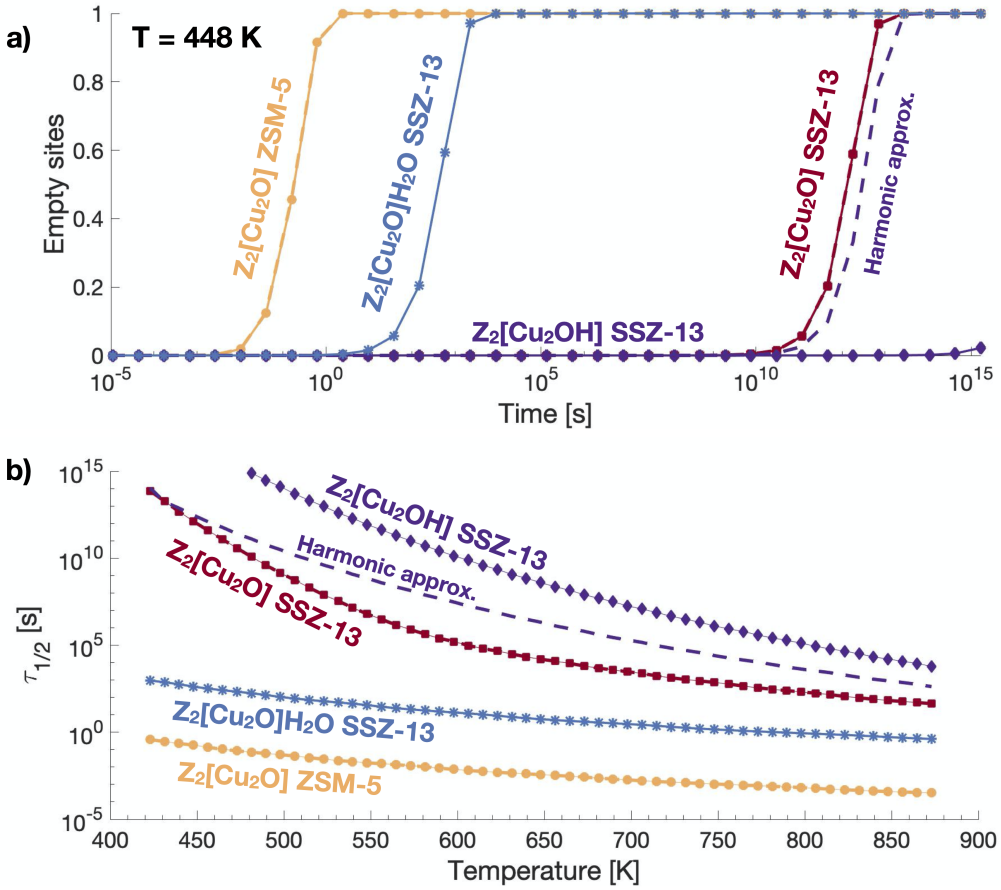

Figure S8: Transient kinetics of the $Z_2[Cu_2O]$ in ZSM-5 (yellow circles), $Z_2[Cu_2O]$ in SSZ-13 (red squares), and $Z_2[Cu_2OH]$ in SSZ-13 (purple diamonds).

CH_3OH desorption.

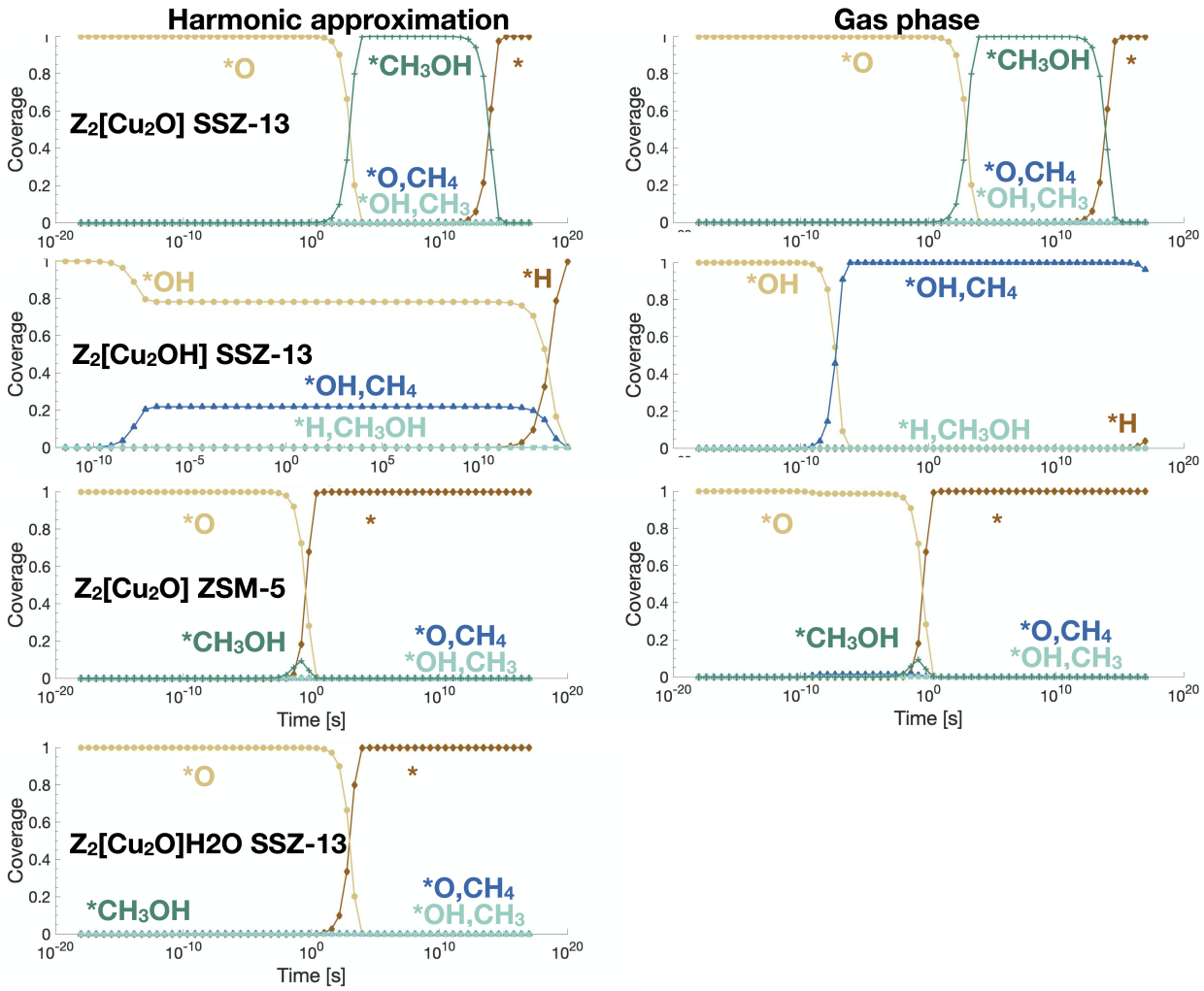

Figure S9: Coverages for the four systems according to the two different treatments of the entropy. To the left, the harmonic approximation is shown, and to the right, is the gas-phase treatment. The top row shows the $Z_2[Cu_2O]$ in SSZ-13, the second $Z_2[Cu_2OH]$ in SSZ-13, the third $Z_2[Cu_2O]$ in ZSM-5, and the bottom $Z_2[Cu_2O]H_2O$ in SSZ-13.

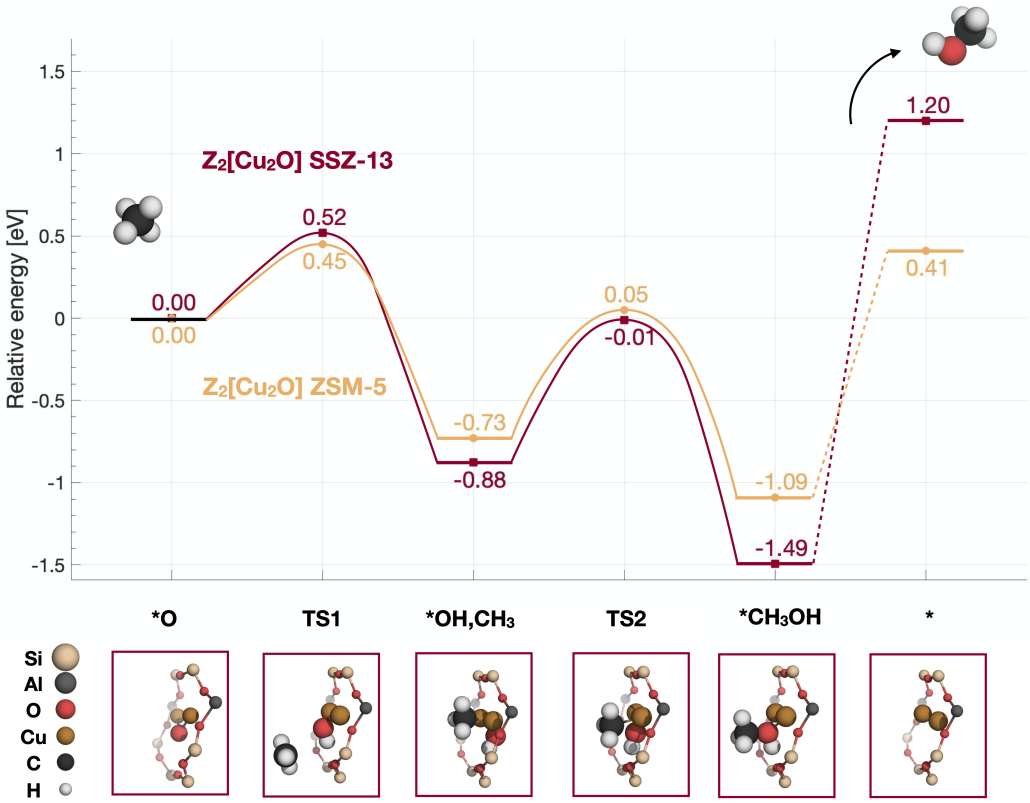

Figure S10: Reaction mechanism over $Z_2[Cu_2O]$ in ZSM-5 (yellow circles) and SSZ-13 (red squares). The reaction over both systems proceed through the same basic steps, the structures provided are those present in SSZ-13. All energies are in eV.